Inorganic Chemistry

ARTICLE

pubs.acs.org/IC

$RbCN_3H_4$: The First Structurally Characterized Salt of a New Class of Guanidinate Compounds

Veronika Hoepfner and Richard Dronskowski*

Institute of Inorganic Chemistry, RWTH Aachen University, Landoltweg 1, D-52056 Aachen, Germany

Supporting Information

ABSTRACT: Rubidium guanidinate, $RbCN_3H_4$, was synthesized from guanidine and rubidium hydride, and the crystal structure was determined from powder X-ray diffraction (PXRD) data. $RbCN_3H_4$ crystallizes in the orthorhombic space group *Pnma* (No. 62) with four formula units per cell. The guanidinate anions are arranged in double chains running along the *b* axis, stacked almost perpendicularly to each other to form a three-dimensional network. The rubidium cations, coordinated by 11 N atoms, occupy the vacancies of the network in a zigzag motif along the *b* axis. Because the PXRD structure of the CN_3 core clearly indicates the N-atom functionalities and the location of the H-atom positions, the latter spatial parameters were determined from Perdew–Burke–Ernzerhof generalized gradient approximation (GGA-PBE) density functional theory calculations. The corresponding ν(NH) stretching modes can be observed in the IR spectrum, and the volume chemistry of $RbCN_3H_4$ mirrors the efficient packing of the saltlike phase.

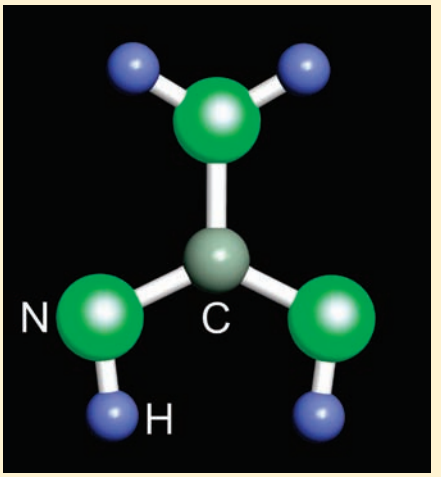

INTRODUCTION

The guanidine molecule, $(NH_2)_2C{=}NH$, is an important ingredient of both organic and inorganic chemistry. Despite its early synthesis in 1861,[1] the elucidation of its crystal structure had to wait for another 148 years.[2] Among its chemical properties, the very strong basic character of guanidine ($pK_B = 0.4$)—thus being one of the strongest organic bases, similar to alkali hydroxides—is certainly worth mentioning,[3] and the basicity goes back to the fact that the molecule eagerly binds one proton to form the mesomerism-stabilized cation $[(NH_2)_3C]^+$.[4] It is therefore not at all surprising that a large number of salts containing the guanidinium cation may be found in the literature, for example, $(NH_2)_3CCl$[5] and $[(NH_2)_3C][HSO_4]$,[6] and the cation has been extensively studied, both experimentally and theoretically. In addition, there is a rich coordination chemistry of *substituted* guanidine ligands, both neutral and negatively charged, together with various metals.[7]

In sharp contrast, guanidine compounds containing a negatively charged, *unsubstituted* guanidinate *anion* are almost unknown, simply because such a strong base does not lend itself to easy deprotonation. There is only one report, by Franklin in 1922, which states the formation of dipotassium guanidinate, $K_2CN_3H_3$, and monosilver guanidinate, $AgCN_3H_4$.[8] According to that pioneering work, the two salts were obtained by the reaction of guanidine nitrate with the metal amide in liquid ammonia, but because of the noncrystallinity of the products, it was impossible to clarify their crystal structures. Instead, the compositions were determined from elemental analysis, namely, the amount of potassium (as K_2SO_4), silver (as AgCl), and nitrogen (Kjeldahl technique) in the two compounds.

We here report on the synthesis and structure determination from powder X-ray diffraction (PXRD) data of the first fully characterized guanidinate compound, $RbCN_3H_4$. With this compound, made by a new synthetic approach, the heretofore almost unexplored class of unsubstituted guanidinate salts is now easily accessible.

EXPERIMENTAL SECTION

Synthesis. Because of the sensitivity of the product and also the starting materials against air and humidity, all experiments were carried out either in a dry argon line or in a glovebox. The syntheses of the educts were performed as described in the literature.[2,9−11] Rubidium guanidinate was synthesized by simply mixing guanidine and rubidium hydride in a 1:1 ratio at room temperature. A substantial gas evolution indicates the start of the reaction, which leads to the colorless title compound in practically quantitative yield:

$$(NH_2)_2C{=}NH(s) + RbH(s) \rightarrow RbCN_3H_4(s) + H_2(g)$$

PXRD. The PXRD data at room temperature were collected with the help of a calibrated STOE STADI2/PL diffractometer with strictly monochromatized Cu $K\alpha_1$ radiation and an image-plate position-

Received: January 31, 2011
Published: March 11, 2011

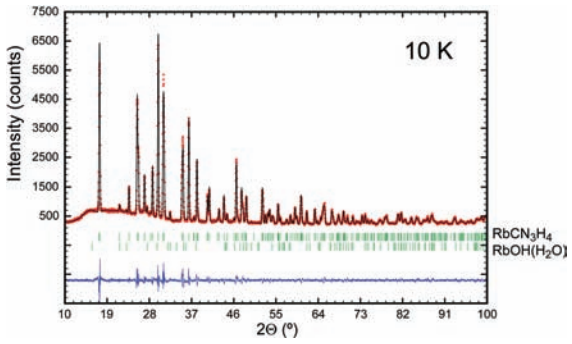

Figure 1. Final Rietveld refinement plot of $RbCN_3H_4$ at T = 10 K, showing the observed (red) and calculated (black) patterns as well as their difference (blue). Green bars indicate the calculated Bragg peaks for both the main phase and the impurity phase $RbOH(H_2O)$.

Table 1. Crystal Data and Structure Refinement Details for $RbCN_3H_4$ at T = 10 K and at Room Temperature

temperature (K)	10	293
empirical formula	$RbCN_3H_4$	
fw (g mol^{-1})	143.5	
cryst syst	orthorhombic	
space group	*Pnma* (No. 62)	
a (Å)	6.9369(4)	6.9969(12)
b (Å)	7.0009(3)	7.0469(12)
c (Å)	7.5087(4)	7.6072(12)
volume (Å^3)	364.657(1)	375.084(4)
Z	4	
calcd density (g cm^{-3})	2.61	2.55
pattern range, 2θ (deg)	6−100	2−125
step scan increment, 2θ (deg)	0.020	0.015
no. of data points	4701	9467
no. of reflns	222	390
no. of restraints	0	2
profile function	pseudo-Voigt	
U	0.17(2)	1.33(7)
V	−0.07(1)	−1.01(7)
W	0.050(2)	0.21(1)
η	0.11(4)	0.71(7)
X	−0.003(1)	−0.009(3)
preferred orientation (011) parameter	0.06(1)	
asymmetry parameter		0.210(7)
R_p[a]	5.42	5.19
R_{Bragg}[b]	3.74	4.40

[a] $R_p = 100(\Sigma|y_i - y_{calc,i}|)/\Sigma|y_i|$. [b] $R_{Bragg} = 100(\Sigma|I_{obs,i} - I_{calc,i}|)/\Sigma|I_{obs,i}|$.

sensitive detector combined with a glass capillary (d = 0.3 mm) as a sample holder; the range of measurement was 2−125° in 2θ with individual steps of 0.015°. The PXRD data at 10 K were collected instead using a Huber G645 diffractometer with strictly monochromatized Cu Kα_1 radiation and a scintillation-counter detector; the range of measurement was 6−100° in 2θ with individual steps of 0.02°. Here, a flat air-proof sample holder was used and was cooled in an evacuated closed-cycle refrigerator.

Structure Determination and Refinement. After PXRD measurement, the positions of 34 strong reflections in the 293 K data were accurately determined for the purpose of indexing, which was then performed using the Visser algorithm and the *ITO*[12] program. Among others, an orthorhombic cell was found that could host between three and four formula units based on the approximate volume increments for Rb^{+13} and molecular guanidine.[2] The *FULLPROF*[14] program was used for the subsequent profile matching and extraction of X-ray intensities. The lowest possible orthorhombic space group ($P222$) was presumed, and a pseudo-Voigt profile function with four terms for correction of the asymmetry in the low-angle region was applied. This resulted in 210 approximate intensities that were subjected to space-group determination using the *HKL* tool as implemented in the *WinGX*[15] program package. The systematic absences immediately pointed toward space group *Pnma* and its noncentrosymmetric subgroup $Pn2_1a$.

Table 2. Spatial and Isotropic Displacement Parameters for $RbCN_3H_4$ at T = 10 K[a]

atom	Wyckoff position	x	y	z	B (Å^2)
Rb	4c	0.0266(3)	$^1/_4$	0.5767(4)	0.71(6)
C	4c	0.3529(27)	$^3/_4$	0.6286(29)	0.3(2)
N1	4c	0.5168(23)	$^1/_4$	0.5205(17)	0.3(2)
N2	8d	0.2996(16)	0.5801(15)	0.6866(14)	0.3(2)
H1	8d	0.448	0.125	0.560	
H2	8d	0.800	0.099	0.214	

[a] The positions of the H atoms were determined from GGA-PBE electronic-structure calculations.

The positions of the Rb and N atoms were determined using direct methods built into the *SHELXS-97* code[16] assuming centrosymmetric *Pnma* symmetry. After the missing C atom was manually placed in the middle of the nitrogen triangle, the crystal structure was successfully refined using *FULLPROF*.[14] Upon refinement, additional Bragg peaks were identified as belonging to the impurity phase $RbOH(H_2O)$,[17] and its contribution (ca. 3%) was simultaneously refined using identical pseudo-Voigt profile parameters. The presence of $RbOH(H_2O)$ results from impure RbH. Fortunately, the quality of the 10 K data allowed the unrestrained refinement of the spatial parameters of the heavy Rb atom and also the much lighter C and N atoms, but for reasons of greater refinement stability, identical isotropic displacement parameters were utilized for C and N. The room temperature data, on the other side, require C−N bond-length restraints and fixed isotropic displacement parameters (1 Å^2); one might well take the view that rigid-body motions, impossible to model using PXRD Rietveld techniques, already persist at 293 K. We therefore restrict ourselves to a discussion of the more accurate 10 K data.

In the final refinements, a preferred orientation parameter on (011) was included in the low-temperature diffraction data while an asymmetry correction was needed for room temperature, a consequence of the two different sample holders. Eventually, the backgrounds of both data sets were smoothed by applying a Fourier filtering (200 points), as was also implemented in *FULLPROF*. The resulting Rietveld plot at 10 K is shown in Figure 1, and the crystal data and refinement details for both temperatures are listed in Table 1.

Despite their excellent quality, the difference Fourier map of the 10 K data did not reveal the positions of the leftover H atoms, very well understandable because of the presence of the heavily scattering Rb neighbor. Nonetheless, the C−N bond lengths immediately allowed one to classify the two different N atoms according to their amino (two bonded H atoms) and imino (one bonded H atom) functionalities. The spatial parameters of the two symmetry-independent H atoms were then straightforwardly calculated from electronic-structure theory (see below). All spatial and isotropic displacement parameters of $RbCN_3H_4$ at a temperature of 10 K are given in Table 2. More details about the crystal-structure investigation may be obtained from Fachinformationszentrum Karlsruhe, Eggenstein-Leopoldshafen, Germany, on quoting the depository number CSD 422591.

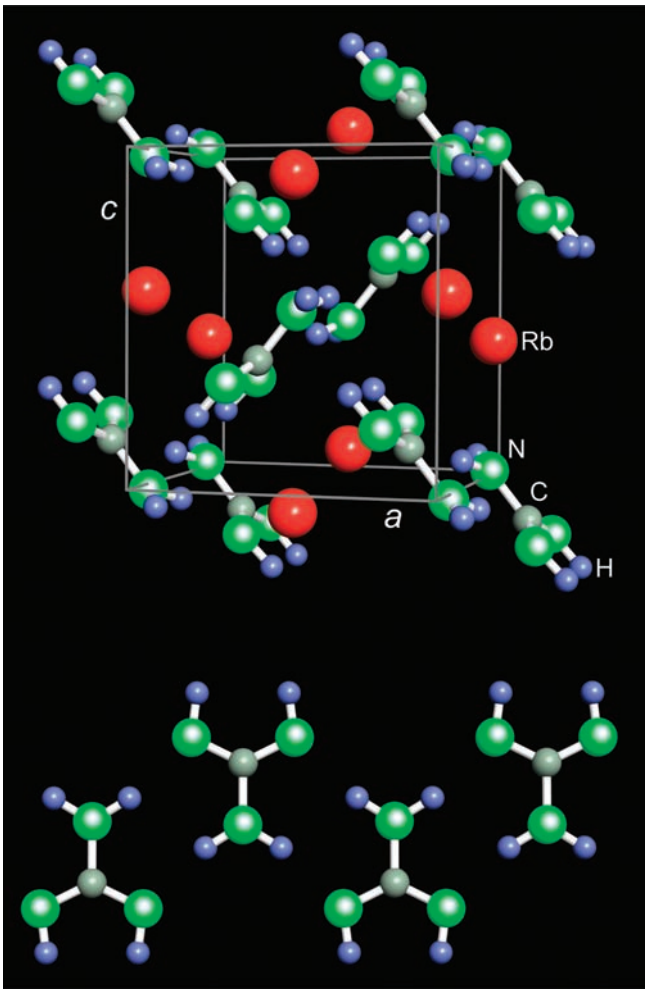

Figure 2. Perspective view[27] into the crystal structure of $RbCN_3H_4$ along the *b* axis (top) and projection of the double chain made up of $[CN_3H_4]^-$ units (bottom). The positions of the H atoms were determined from electronic-structure calculations. Rubidium is in red, nitrogen in green, carbon in black, and hydrogen in blue.

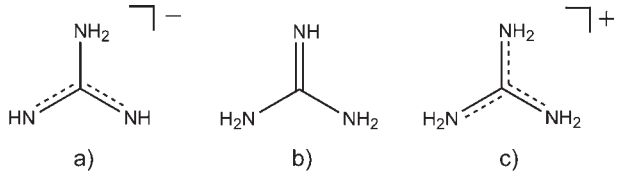

Figure 3. Lewis drawings of (a) the guanidinate anion, (b) the guanidine molecule, and (c) the guanidinium cation. For characteristic bond lengths, see Table 3.

Theory. In order to assist the structural discussion of the guanidine molecule, its cation, and also its anion, high-quality molecular-orbital calculations were carried out using the *Gaussian 03*[18] program suite. All wave-function-based theory was carried out at the MP2(full)6-311+G(d,p) level.

In addition, periodic density functional theory (DFT) calculations were performed using the VASP suite.[19−21] Plane-wave basis sets and PAW potentials[22,23] were applied, with the kinetic energy cutoff set to 400 eV, combined with an exchange-correlation functional of the Perdew−Burke−Ernzerhof generalized gradient approximation (GGA-PBE) type.[24] Integration in the Brillouin zone was done using the improved tetrahedron method[25] on a 5 × 6 × 6 set of Monkhorst−Pack *k* points.[26] To calculate the site parameters of the H atoms, the space-group symmetry, lattice parameters, and all non-H-atom positions (Rb, C, and N) were locked to their experimental values. Then, the approximate positions of the amino- and imino-bonded H atoms were optimized from variational electronic-structure theory (see also the discussion) until vanishing interatomic forces were achieved.

Table 3. Comparison of Experimentally Determined and Theoretically Calculated C−N Bond Lengths (Å) of a Guanidinate Anion (Left), a Neutral Guanidine (Middle), and a Guanidinium Cation (Right) as a Function of the Bond Order[a]

	$RbCN_3H_4$ (this work)		CN_3H_5[2]		CN_3H_6Cl[5]	
bond order	10 K	calcd	100 K	calcd	RT	calcd
1.0	1.44	1.437	1.37	1.394		
1.5	1.32	1.336			1.33	1.336
2.0			1.30	1.292		

[a] The calculated values for all three species were obtained with the *Gaussian 03* program at the MP2(full)6-311+G(d,p) level of theory.

RESULTS AND DISCUSSION

Rubidium guanidinate has been synthesized in quantitative yield, and its crystal structure was determined from PXRD data at room temperature and 10 K (Tables 1 and 2). There is no evidence for any phase transition between these two temperatures. In addition, a PXRD scan between 10 and 430 °C shows that decomposition, but not melting, occurs around 140 °C. We conclude that rubidium guanidinate is stable up to this temperature.

$RbCN_3H_4$ crystallizes in the orthorhombic space group *Pnma* (No. 62) with four formula units per unit cell, as depicted[27] in the upper part of Figure 2. The substructure made up from the complex $[CN_3H_4]^-$ anions corresponds to double chains which run along the *b* axis, and two such neighboring chains are oriented almost perpendicular to each other to eventually generate the three-dimensional guanidinate network. Within each double chain, a projection of which is shown in the bottom part of Figure 2, every second guanidinate group is shifted slightly out of the plane, by 0.412(8) Å, making the chains a bit noncoplanar.

The rubidium ions occupy the vacancies of the guanidinate network, and the motif corresponds to zigzag "chains" along the *b* axis, with Rb^+−Rb^+ distances of 3.704(1) Å in the "chains" and 4.339(2) Å between them, significantly larger than twice the effective ionic radius of Rb^+ (1.69 Å) for 11-fold coordination.[28] Each Rb^+ is coordinated by 11 N atoms between 2.98 and 3.55 Å, and Schwarzenbach's method[29] arrives at a likewise large effective coordination number of 8.95, not at all surprising for the voluminous Rb atom.

As was alluded to already, the excellent low-temperature data quality allowed one to characterize the functionality of the guanidinate anion solely on the basis of the C−N bond lengths, even without prior knowledge of the H-atom positions. For illustration, Figure 3 presents schematic drawings of (a) the guanidinate anion, (b) the guanidine molecule, and (c) the guanidinium cation. The corresponding C−N bond lengths are provided in Table 3, both using experimental and theoretical [at the MP2(full)6-311+G(d,p) level] values. For the neutral

dx.doi.org/10.1021/ic2002089 |*Inorg. Chem.* 2011, 50, 3799–3803

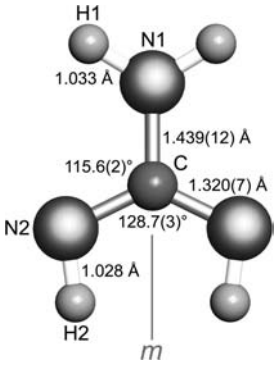

Figure 4. Molecular structure of the guanidinate anion at $T = 10$ K. The C and N positions were experimentally determined, while the positions of the H atoms were calculated from GGA-PBE DFT. A vertical mirror plane *m* runs through N1 and C.

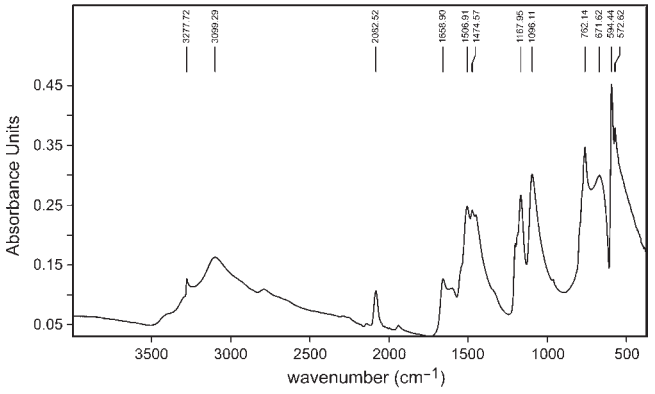

Figure 5. IR spectrum of $RbCN_3H_4$ taken at room temperature.

guanidine molecule (middle entries), the central C═N double bond is clearly shorter than the two outer C−N single bonds. This obvious difference no longer persists in the mesomerism-stabilized guanidinium cation (right entries), with a 1.5 bond order throughout the molecule and C−N ≈ 1.33 Å. The latter shorter bond length is found experimentally for the C−N2 combination in $RbCN_3H_4$, and an enlarged single-bond length (≈1.44 Å) results for the C−N1 combination. Thus, N1 is clearly identified as the amino N atom, bonded to two H atoms, and N2 is the imino N atom, bonded to one H atom. This assignment is also verified by the quantum-chemical calculation on the heretofore structurally unknown $[CN_3H_4]^-$ anion because it arrives at practically the same bond lengths (Table 3, left entries); the slightly enlarged C−N1 bond length seen both experimentally and theoretically probably mirrors the anionic charge.

By using that amino/imino assignment, periodic DFT calculations allowed one to easily optimize the spatial parameters of the bonded H atoms, given in Table 2, and thereby corroborate the differing N functionalities; an alternative but incorrect starting structure (for example, with the N1 amino atom carrying only one H atom and one of the two N2 imino atom carrying two H atoms instead) is less stable by an enormous 111 kJ mol^{-1}. Figure 4 depicts the entire guanidinate anion in greater detail. A vertical mirror plane runs through the N1 and C atoms, and the bond lengths are 1.44 Å for C−N1 and 1.32 Å for the C−N2 combination. Likewise, the N2−C−N2 angle is larger (ca. 129°) than that of N1−C−N2 (ca. 116°), thereby reflecting the greater (1.5) bond order of C−N2. Both N−H bond distances are calculated as 1.03 Å, but it is only H1 that points toward a neighboring N2 atom at a distance of 2.01 Å (see Figure 2, bottom). One may assume the presence of such N1−H1···N2 hydrogen bridges, in particular because the N1···N2 distance, ca. 3.02 Å, is similar to the N···N donor−acceptor distances in molecular guanidine.[2] This notion is corroborated by the IR spectrum of $RbCN_3H_4$ (Figure 5), which exhibits two intense absorptions at 3278 and 3099 cm^{-1}, assignable to the ν(NH) stretching modes. The broad nature of these absorptions indicates the presence of such hydrogen bonds between opposite imino and amino groups, but no further differentiation can be done. Similar findings were observed in the spectrum of guanidine and the guanidinium cation, each showing three very broad signals between 3419 and 3140 cm^{-1}, denoted as ν(N−H···N) absorptions.[30] Finally, the CN_3 core of the anion is perfectly planar within two standard deviations because the C atom does not deviate more than 0.017(10) Å from the surrounding nitrogen triangle.

The volume chemistry of rubidium guanidinate is surprising, but only at first sight. The compound has a molar volume of 55 cm^3 mol^{-1}, which, given the Rb^+ volume increment,[13] translates into a rather compact 35 cm^3 mol^{-1} for $[CN_3H_4]^-$. Thus, the anion looks *smaller* than the neutral molecule CN_3H_5[2] by 11 cm^3 mol^{-1}, despite the fact that the intermolecular C−N bond lengths are *larger*; note that the volume increment of H is zero.[13] Because of these larger C−N bond lengths, a (slightly) larger van der Waals surface of $[CN_3H_4]^-$ should result compared with the one of CN_3H_5. Nonetheless, the smaller volume increment clearly indicates that $RbCN_3H_4$ is more efficiently *packed* than molecular guanidine or even corresponding salts such as guanidinium chloride.[5]

CONCLUSION

The first guanidinate compound of rubidium, $RbCN_3H_4$, has been synthesized, and the structure was solved from PXRD data. Because the positions of the heavy-atom Rb and also C and N were refinable from the low-temperature (10 K) data, the nitrogen assignment (amino and imino functionality) was straightforward, thereby allowing calculation of the H-atom positions on the basis of GGA-PBE DFT. Neutron-diffraction measurements on single crystals would be required to collect anisotropic displacement parameters for all atoms, needed for a full rigid-body correction of the anionic motion and, thus, perfectly accurate C−N and N−H bond lengths at room temperature. The volume chemistry of $RbCN_3H_4$ mirrors the efficient packing of the saltlike compound.

ASSOCIATED CONTENT

Supporting Information. X-ray crystallographic data in CIF format. This material is available free of charge via the Internet at http://pubs.acs.org.

AUTHOR INFORMATION

Corresponding Author
*E-mail: drons@HAL9000.ac.rwth-aachen.de.

■ ACKNOWLEDGMENT

We thank Arno Görne for his experimental work and the high-performance computing center of Forschungszentrum Jülich for providing us with large amounts of CPU time.

■ REFERENCES

(1) Strecker, A. *Liebigs Ann. Chem.* **1861**, *118*, 151.
(2) Yamada, T.; Liu, X.; Englert, U.; Yamane, H.; Dronskowski, R. *Chem.—Eur. J.* **2009**, *15*, 5651.
(3) Angyal, S. J.; Warburton, W. K. *J. Chem. Soc.* **1951**, 2492.
(4) Gobbi, A.; Frenking, G. *J. Am. Chem. Soc.* **1993**, *115*, 2362.
(5) Haas, D. J.; Harris, D. R.; Mills, H. H. *Acta Crystallogr.* **1965**, *19*, 676.
(6) Dera, P.; Katrusiak, A.; Szafrański, M. *Polish J. Chem.* **2000**, *74*, 1637.
(7) Bailey, P. J.; Pace, S. *Coord. Chem. Rev.* **2001**, *214*, 91.
(8) Franklin, E. C. *J. Am. Chem. Soc.* **1922**, *44*, 486.
(9) Jung, R. P. Über ternäre Alkalimetall-Übergangsmetall-Hydride. Dissertation, RWTH Aachen University, Aachen, Germany, 1991.
(10) Jansen, K. Zur Synthese and Struktur ternärer Erdalkalimetall-Übergangsmetall-Hydride. Dissertation, RWTH Aachen University, Aachen, Germany, 1990.
(11) Bronger, W.; Auffermann, G.; Müller, P. *J. Less-Common Met.* **1988**, *142*, 243.
(12) Visser, J. W. *J. Appl. Crystallogr.* **1969**, *2*, 89.
(13) Biltz, W. *Raumchemie der festen Stoffe*; Verlag von Leopold Voss: Leipzig, Germany, 1934.
(14) J. Rodríguez-Carvajal *FULLPROF2000*, version 3.2; Laboratoire Léon Brillouin: Gif-sur-Yvette Cedex, France, 1997.
(15) Farrugia, L. J. *J. Appl. Crystallogr.* **1999**, *32*, 837.
(16) Sheldrick, G. M. *Acta Crystallogr., Sect. A* **2008**, *64*, 112.
(17) Jacobs, H.; Tacke, T.; Kockelkorn, J. *Z. Anorg. Allg. Chem.* **1984**, *516*, 67.
(18) Frisch, M. J.; Trucks, G. W.; Schlegel, H. B.; Scuseria, G. E.; Robb, M. A.; Cheeseman, J. R.; Montgomery, J. A., Jr.; Vreven, T.; Kudin, K. N.; Burant, J. C.; Millam, J. M.; Iyengar, S. S.; Tomasi, J.; Barone, V.; Mennucci, B.; Cossi, M.; Scalmani, G.; Rega, N.; Petersson, G. A.; Nakatsuji, H.; Hada, M.; Ehara, M.; Toyota, K.; Fukuda, R.; Hasegawa, J.; Ishida, M.; Nakajima, T.; Honda, Y.; Kitao, O.; Nakai, H.; Klene, M.; Li, X.; Knox, J. E.; Hratchian, H. P.; Cross, J. B.; Bakken, V.; Adamo, C.; Jaramillo, J.; Gomperts, R.; Stratmann, R. E.; Yazyev, O.; Austin, A. J.; Cammi, R.; Pomelli, C.; Ochterski, J. W.; Ayala, P. Y.; Morokuma, K.; Voth, G. A.; Salvador, P.; Dannenberg, J. J.; Zakrzewski, V. G.; Dapprich, S.; Daniels, A. D.; Strain, M. C.; Farkas, O.; Malick, D. K.; Rabuck, A. D.; Raghavachari, K.; Foresman, J. B.; Ortiz, J. V.; Cui, Q.; Baboul, A. G.; Clifford, S.; Cioslowski, J.; Stefanov, B. B.; Liu, G.; Liashenko, A.; Piskorz, P.; Komaromi, I.; Martin, R. L.; Fox, D. J.; Keith, T.; Al-Laham, M. A.; Peng, C. Y.; Nanayakkara, A.; Challacombe, M.; Gill, P. M. W.; Johnson, B.; Chen, W.; Wong, M. W.; Gonzalez, C.; Pople, J. A. *Gaussian 03*, revision D.02; Gaussian, Inc.: Wallingford, CT, 2004.
(19) Kresse, G.; Hafner, J. *Phys. Rev. B* **1993**, *47*, 558; *Phys. Rev. B* **1994**, *49*, 14251.
(20) Kresse, G.; Furthmüller, J. *Comput. Mater. Sci.* **1996**, *6*, 15.
(21) Kresse, G.; Furthmüller, J. *Phys. Rev. B* **1996**, *54*, 11169.
(22) Blöchl, P. E. *Phys. Rev. B* **1994**, *50*, 17953.
(23) Kresse, G.; Joubert, D. *Phys. Rev. B* **1999**, *59*, 1758.
(24) Perdew, J. P.; Burke, K.; Ernzerhof, M. *Phys. Rev. Lett.* **1996**, *77*, 3865.
(25) Blöchl, P. E.; Jepsen, O.; Andersen, O. K. *Phys. Rev. B* **1994**, *49*, 16223.
(26) Monkhorst, H. J.; Pack, J. D. *Phys. Rev. B* **1976**, *13*, 5188.
(27) Ozawa, T. C.; Kang, S. J. *J. Appl. Crystallogr.* **2004**, *37*, 679.
(28) Shannon, R. D. *Acta Crystallogr., Sect. A* **1976**, *32*, 751.
(29) Brunner, G. O.; Schwarzenbach, D. *Z. Kristallogr.* **1971**, *133*, 127.
(30) Jones, W. J. *Trans. Faraday Soc.* **1959**, *55*, 524.